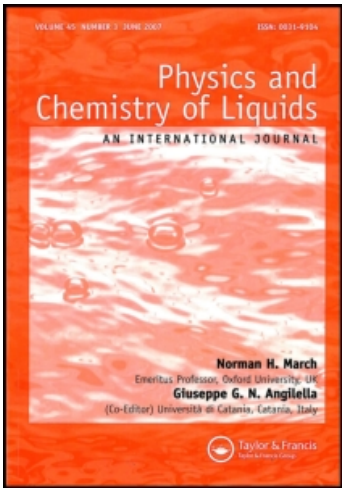

Physics and Chemistry of Liquids
Publication details, including instructions for authors and subscription information:
http://www.informaworld.com/smpp/title~content=t713646857

Spectrochemical Investigations of Preferential Solvation. Part 3. Extension of the Khossravi-Connors-Skwierczynski Two-Step Competitive Solvation Model to Fluorescence Emission Behavior of Polycyclic Aromatic Hydrocarbon Solvent Polarity Probes Dissolved in Binary Solvent Mixtures

William E. Acree Jr.[a]; Sheryl A. Tucker[a]; Denise C. Wilkins[a]; Jason M. Griffin[a]
[a] Department of Chemistry, University of North Texas, Denton, Texas, USA

To cite this Article Acree Jr., William E. , Tucker, Sheryl A. , Wilkins, Denise C. and Griffin, Jason M.(1995) 'Spectrochemical Investigations of Preferential Solvation. Part 3. Extension of the Khossravi-Connors-Skwierczynski Two-Step Competitive Solvation Model to Fluorescence Emission Behavior of Polycyclic Aromatic Hydrocarbon Solvent Polarity Probes Dissolved in Binary Solvent Mixtures', Physics and Chemistry of Liquids, 30: 2, 79 — 93
To link to this Article: DOI: 10.1080/00319109508046427
URL: http://dx.doi.org/10.1080/00319109508046427

Phys. Chem. Liq., 1995, Vol. 30, pp. 79–93
Reprints available directly from the publisher
Photocopying permitted by license only

SPECTROCHEMICAL INVESTIGATIONS OF PREFERENTIAL SOLVATION. PART 3. EXTENSION OF THE KHOSSRAVI-CONNORS-SKWIERCZYNSKI TWO-STEP COMPETITIVE SOLVATION MODEL TO FLUORESCENCE EMISSION BEHAVIOR OF POLYCYCLIC AROMATIC HYDROCARBON SOLVENT POLARITY PROBES DISSOLVED IN BINARY SOLVENT MIXTURES

WILLIAM E. ACREE, JR., * SHERYL A. TUCKER,
DENISE C. WILKINS and JASON M. GRIFFIN

Department of Chemistry University of North Texas,
Denton, Texas 76203–5068 (USA)

(Received 26 January 1995)

The Khossravi-Connors-Skwierczynski step-wise competitive exchange model, which has previously led to successful descriptive expressions for solvent effects on solubility, surface tension and molecular complex formation, is modified to model fluorescence emission behavior of polycyclic aromatic hydrocarbon solutes dissolved in binary solvent mixtures. Expressions are derived for calculating numerical values of the various step-wise exchange equilibrium constants from measured emission intensity ratios in mixed solvents and from measured absolute emission intensities in both pure solvents. Computation procedure is illustrated using measured fluorescence properties of pyrene, benzo[e]pyrene, benzo[ghi]perylene, coronene, methylcoronene and 1,2-dimethylcoronene in *n*-heptane + 1,4-dioxane and *n*-heptane + tetrahydrofuran mixtures. Also discussed are similarities and differences between the newly-derived expressions and ones based upon a recently published spectrofluorometric probe method, and the special conditions under which both models become mathematically equivalent.

KEY WORDS: Fluorescence probe methods, polycyclic aromatic hydrocarbons, binary solvent mixtures.

INTRODUCTION

Spectroscopic probe techniques provide a convenient experimental means to study preferential solvation, which can be used to support (or perhaps to discredit) interpretations derived from calorimetric and other thermodynamic data. Preferential solvation arises whenever the proportion of molecules of any given solvent component within the probe's solvational microsphere is not equal to its bulk mole fraction composition. "True preferential solvation" is extremely difficult, if not impossible, to

* To whom correspondence should be addressed.

model rigorously because there is no guarantee that probe-solvent A and probe-solvent B molecular interactions remain independent of other solvent molecules within the solvational sphere. Solvent-solvent interactions may lead to synergistic effects. Although not always stated explicitly, most published spectroscopic probe techniques[1-8] assume a more idealized situation where solvent-solvent interactions are neglected and the measured spectral response, R, in a binary solvent mixture is given by

$$R = Y_A R_A^0 + (1 - Y_A) R_B^0 \tag{1}$$

a weighted local mole fraction or volume fraction average of the probe's spectral responses in the two pure solvents, R_A^0 and R_B^0. Here Y_A and $1-Y_A$ refer to the solvational sphere composition, which may be quite different from the overall bulk liquid-phase composition, X_A and $1-X_A$. Rigorous derivation of Eqn. 1 from fundamental spectroscopic principles requires that one assume that the solvational sphere around every solute probe is solvated by only one type of solvent molecule. More sophisticated approaches[9] also incorporate molecular size disparity and permit the solute to have a different coordination number in the binary solvent than in the pure solvents.

Modification of Eqn. 1 for a polycyclic aromatic hydrocarbon (*PAH*) solvatochromic probe molecule dissolved in a binary mixture (or if one prefers, two different solvational microphases) is relatively straightforward. Each solvated fluorophore contributes to the observed fluorescence signal, F_{obs}, at each emission wavelength scanned. Emission intensities are additive at each wavelength. In the case of a polycyclic aromatic hydrocarbon solvent polarity probe such as pyrene, the calculated I_1/I_3 emission intensity ratio is[10]

$$I_1/I_3 \approx [Y_A I_{1,\text{phase}A} + (1 - Y_A) I_{1,\text{phase}B}]/[Y_A I_{3,\text{phase}A} + (1 - Y_A) I_{3,\text{phase}B}] \tag{2}$$

Here, [Fluoro] is the total stoichiometric fluorophore molar concentration, and Y_A and $1-Y_A$ represent the mole number fraction of each type of solvated fluorophore, *i.e.*, Y_A = [Fluoro A]/[Fluoro] and $1-Y_A$ = [Fluoro B]/[Fluoro]. Inherent in the above treatment is the underlying assumption that neither microphase forms a nonfluorescent association complex with the fluorophore. If such complexation does occur, then Eqn. 2 describes only the fraction of the solute molecules that actually fluoresce. It is also assumed that both the one and three band emission wavelengths are medium independent, which is not strictly true, hence the approximately equal to sign is used. Rigorous applications require that intensity measurements be made at two fixed emission wavelengths. Acree *et al.*[10] previously showed that Eqn. 2 does accurately reproduce fluorescence behavior of pyrene, benzo[ghi]perylene, coronene and benzo[e]pyrene dissolved in *n*-heptane + 1,4-dioxane and *n*-heptane + tetrahydrofuran mixtures. Calculated Y_A values indicated that the polycyclic aromatic hydrocarbon solute probe was preferentially solvated by the nonpolar *n*-heptane cosolvent, with the degree of preferential solvation decreasing with increased PAH molecular size.

Preferential solvation models, like Eqn. 1, represent only one of many possible approaches for mathematically describing how a chromophore's/fluorophore's

spectroscopic behavior varies with binary solvent composition. Skwierczynski and Connors[11] recently proposed a two-step competitive exchange process to model solute–solvent solvation effects as follows:

$$RA_2 + B \rightleftharpoons RAB + A \quad K_1 = X_{RAB} X_A / (X_{RA2} X_B)$$

$$RAB + B \rightleftharpoons RB_2 + A \quad K_2 = X_{RB2} X_A / (X_{RAB} X_B)$$

Fractions of the three solvational species are defined by:

$$F_{RAA} = X_A^2 / (X_A^2 + K_1 X_A X_B + K_1 K_2 X_B^2) \tag{3}$$

$$F_{RAB} = K_1 X_A X_B / (X_A^2 + K_1 X_A X_B + K_1 K_2 X_B^2) \tag{4}$$

$$F_{RBB} = K_1 K_2 X_B^2 / (X_A^2 + K_1 X_A X_B + K_1 K_2 X_B^2) \tag{5}$$

where X_A and X_B refer to bulk mole fractions of the two solvent components. The authors assumed that the reciprocal of the maximum absorption wavelength [λ_{max} (nm); E_T (kcal mol^{-1}) = 28591.5/λ_{max}(nm)] of the Dimroth–Reichardt betaine dye E_T was a weighted average of the contributions or fractions of dye by the various solvated species

$$E_T(X_B) = F_{RAA} E_T(RA_2) + F_{RAB} E_T(RAB) + F_{RBB} E_T(RB_2) \tag{6}$$

Spectral properties of solvational species RA_2 and RB_2 were determined experimentally by recording the absorption spectrum of the dye in each pure solvent. The E_T value of the "mixed" solvational species RAB was approximated as

$$E_T(RAB) = (1/2)\,[E_T(RA_2) + E_T(RB_2)] \tag{7}$$

a simple arithmetic average of solute properties in the two pure solvents. Through a series of algebraic manipulations, Eqn. 6 was rearranged to a more convenient form

$$[E_T(X_B) - E_T(RA_2)]/[E_T(RB_2) - E_T(RA_2)] = [0.5 K_1 X_A X_B + K_1 K_2 X_B^2] \div (X_A^2 + K_1 X_A X_B + K_1 K_2 X_B^2) \tag{8}$$

so as to enable computation of K_1 and K_2 by least squares regression curvefitting techniques. The simple solvational model was found to accurately describe measured E_T data in 17 different binary aqueous–organic mixtures using either one or two curve-fit parameters. Several earlier papers documented that the model provided excellent descriptions of solvent effects, in aqueous–organic mixtures, on solubility,[12,13] surface tension,[14] and molecular complex formation.[15,16]

To provide a better understanding of spectrofluorometric probe methods and solvational phenomena, we examine in this paper the applicability of the Khossravi-Connors-Skwierczynski two-step competitive exchange model for quantitatively

describing fluorescence behavior of PAH solvatochromic probe molecules. Expressions are derived for determining the K_1 and K_2 step-wise exchange constants from the PAH's measured I_1/I_3 (or I_1/I_2, or I_1/I_4) emission intensity ratio in two binary solvent mixtures, and from measured I_1 and I_3 band intensities in both pure solvents. Computational procedure is illustrated using experimental fluorescence properties of pyrene (Py), benzo[ghi]perylene (BPe), benzo[e]pyrene (BePy), coronene (Co), methylcoronene (MeCo) and 1,2-dimethylcoronene (DiMeCo) dissolved in binary *n*-heptane + 1,4-dioxane and *n*-heptane + tetrahydrofuran solvent mixtures. The six aforementioned PAH solutes exhibit solvatochromic behavior as a result of selective emission intensity enhancement with increasing solvent polarity.

MATERIALS AND METHODS

Methylcoronene and 1,2-dimethylcoronene were obtained by a catalytic hydrocracking process[17], purified by chromatography and characterized by standard methods including NMR. Coronene, benzo[e]pyrene, pyrene and benzo[ghi]perylene were purchased commercially from Aldrich Chemical Company in the highest purity available (99 + %). The latter two solutes were recrystallized several times from absolute ethanol before use. Stock solutions were prepared by dissolving solutes in dichloromethane. Known aliquots of the stock solutions were transferred into test tubes, allowed to evaporate, and diluted quantitatively with the solvent of interest. Final solute concentrations of 10^{-5} Molar (or less) were sufficiently dilute to minimize inner-filtering artifacts. Solvents were of HPLC, spectroquality or AR grade, purchased commercially from Aldrich Chemical Company, and the resulting solutions were optically dilute (absorbance $cm^{-1} < 0.01$) at all wavelengths so as to minimize undesired primary and secondary inner-filtering artifacts.[18] Gas chromatographic analysis showed solvent purities to be 99.95 % (or better). Binary solvent mixtures were prepared volumetrically with burettes so that stoichiometric mole and volume fraction compositions could be calculated to $\pm$ 0.01 or better.

Absorption spectra were recorded on a Bausch and Lomb Spectronic 2000 and a Hewlett-Packard 8450A photo-diode array spectrophotometer in the usual manner. The fluorescence spectra were run on a Shimadzu RF-5000U spectrofluorometer with the detector set at high sensitivity. Solutions were excited at 338 nm (Py), 380 nm (BPe), 334 nm (Co), 335 nm (BePy), 340 nm (MeCo) and 305 nm (DiMeCo). Fluorescence data were accumulated in a quartz 1-cm^2 cuvette at 19 °C, ambient room temperature, with excitation and emission slit width settings of 15 nm and 3 nm, respectively. Emission spectra obtained represent a single scan which was then solvent blank corrected and verified by repetitive measurements.

RESULTS AND DISCUSSION

The various PAH polarity scales, defined as ratios of emission intensities of select vibronic bands,[19-26] provide a quantitative measure of solvent polarity. Figure 1 depicts the variation of intensity ratios of Py, BPe, Co, MeCo, DiMeCo and BePy

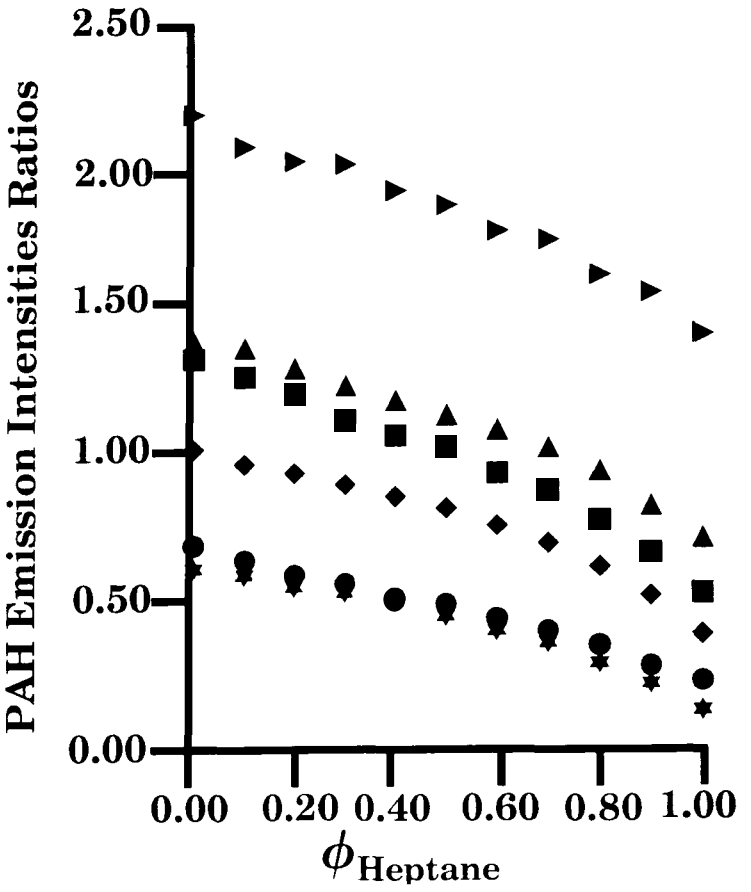

Figure 1 Variation of fluorescence emission intensity ratios with stoichiometric volume fraction composition for pyrene (Py, ■), benzo[e]pyrene (BePy, ●), benzo[ghi]perylene (BPe, ◆), coronene (Co, ★), methylcoronene (MeCo, ▲) and 1,2-dimethylcoronene (DiMeCo, ▻) dissolved in binary *n*-heptane + 1,4-dioxane solvent mixtures. Specific emission intensity ratios used were: Py = *I*(circa 371 nm)/III (*circa* 382 nm); Co = I(*circa* 426 nm)/III (*circa* 444 nm); BPe = I(*circa* 405 nm)/III(*circa* 417 nm); BePy = I (*circa* 376 nm)/II(*circa* 386 nm); MeCo = I(*circa* 427 nm)/III(*circa* 446 nm); and DiMeCo = I(*circa* 430 nm) /III(*circa* 448 nm). Emission band wavelengths are solvent dependent and may differ slightly from one spectrofluorometer to another because of errors or uncertainties in the emission monochromator calibration.

with stoichiometric volume fraction composition for the binary *n*-heptane + 1,4-dioxane solvent system. Reproducibility of each measured numerical value is estimated to be ± 0.02 based upon replicate measurements for select binary mixtures, which were independently prepared. Examination of Figure 1 reveals that the experimental intensity ratios are not a simple stoichiometric volume fraction average of the pure solvent values. Most values lie above the line connecting the two and values.

From a theoretical standpoint, variation of emission intensity ratios with solvent composition can be mathematically modeled in a relatively straightforward manner. The solvational sphere around every PAH fluorophore is assumed to be solvated by

only two solvent molecules, as depicted in the Khossravi-Connors-Skwierczynski two-step competitive solvation scheme. As discussed elsewhere,[29] molecules in most organic mixtures are believed to have an essentially constant coordination number. If the molecular volumes of the two solvent components, V_A and V_B, differ then the substitution of solvent B for A (considered to be the smaller of the two solvent components) in the coordination shell of an infinitely dilute solute would result in a reduction in the number of actual molecular contacts the solute experiences. For molecules of not too great of size disparity, the molecular volume ratio of V_B/V_A may be taken as the parameter that determines the relative number of whole molecular contacts.[30] While two is generally smaller than coordination numbers employed in most thermodynamic solution models, it must be remembered that one more equilibrium constant is required for each additional solvational species included in the basic model.

Each solvated fluorophore contributes to the observed fluorescence signal, F_{obs}, at each emission wavelength scanned

$$F_{obs} = K'_{\text{fluoro}\,RAA}(P_o - P_{\text{fluoro}\,RAA}) + K'_{\text{fluoro}\,RBB}(P_o - P_{\text{fluoro}\,RBB}) + K'_{\text{fluoro}\,RAB}(P_o - P_{\text{fluoro}\,RAB}) \tag{9}$$

where P_o refers to the intensity of the incoming monochromatic excitation radiation and $(P_o - P_{\text{fluoro}\,i})$ is the amount of radiation absorbed by solvated fluorophore type i. The three proportionality constants, $K'_{\text{fluoro}\,RAA}$, $K'_{\text{fluoro}\,RBB}$ and $K'_{\text{fluoro}\,RAB}$, depend upon the various optical component placements within the instrument, detector response/efficiency, and quantum yield of the given solvated fluorophore. The Beer-Lambert law relates the intensity of unabsorbed excitation radiation, $P_{\text{fluoro}\,i}$, to the molar concentration of the fluorophore and molar extinction, $\epsilon_{\text{fluoro}\,i}$, as follows

$$P_{\text{fluoro}\,i} = P_o\, 10^{-b\epsilon_{\text{fluoro}\,i}[\text{Fluoro}\,i]} \tag{10}$$

Substitution of Eqn. 10 into Eqn. 9 gives

$$F_{obs} = K'_{\text{fluoro}\,RAA}\, P_o(1 - 10^{-b\epsilon_{\text{fluoro}\,RAA}[\text{Fluoro}\,RA_2]}) + K'_{\text{fluoro}\,RAB}\, P_o(1 - 10^{-b\epsilon_{\text{fluoro}\,RAB}[\text{Fluoro}\,RAB]}) + K'_{\text{fluoro}\,RBB} P_o(1 - 10^{-b\epsilon_{\text{fluoro}\,RBB}[\text{Fluoro}\,RB_2]}) \tag{11}$$

which can be expanded as a Maclaurin power series to yield

$$F_{obs} = K'_{\text{fluoro}\,RAA} P_o \{2.303 b\epsilon_{\text{fluoro}\,RAA}[\text{Fluoro}\,RA_2] - (2.303 b\epsilon_{\text{fluoro}\,RAA}[\text{Fluoro}\,RA_2])^2/2! + (2.303\, b\epsilon_{\text{fluoro}\,A}[\text{Fluoro}\,RA_2])^3/3! - \ldots\} + K'_{\text{fluoro}\,RAB} P_o \{2.303\, b\epsilon_{\text{fluoro}\,RAB}[\text{Fluoro}\,RAB] - (2.303\, b\epsilon_{\text{fluoro}\,RAB}[\text{Fluoro}\,RAB])^2/2! + (2.303\, b\epsilon_{\text{fluoro}\,RAB}[\text{Fluoro}\,RAB])^3/3! - \cdots\}$$

$$+ K'_{\text{fluoro } RBB} P_o \{2.303\, b\epsilon_{\text{fluoro } RBB}[\text{Fluoro } RB_2] - (2.303\, b\epsilon_{\text{fluoro } RBB}[\text{Fluoro } RB_2])^2/2! + (2.303\, b\epsilon_{\text{fluoro } RBB}[\text{Fluoro } RB_2])^3/3! - \cdots\} \quad (12)$$

For every dilute solutions where $2.303\, b\epsilon_{\text{fluoro } i}[\text{Fluoro i}] < 0.05$, the higher-order terms are negligible. Performing this simplification, the measured emission is

$$\begin{aligned} F_{\text{obs}} = {} & 2.303\, K'_{\text{fluoro } RAA} P_o\, b\epsilon_{\text{fluoro } RAA} F_{RAA}[\text{Fluoro}] \\ & + 2.303\, K'_{\text{fluoro } RAB} P_o\, b\epsilon_{\text{fluoro } RAB} F_{RAB}[\text{Fluoro}] \\ & + 2.303\, K'_{\text{fluoro } RBB} P_o b\epsilon_{\text{fluoro } RBB} F_{RBB}[\text{Fluoro}] \end{aligned} \quad (13)$$

whenever expressed in terms of the total stoichiometric fluorophore concentration, [Fluoro]. Here, F_{RAA}, F_{RAB} and F_{RBB} represent the mole number fraction of each type of solvated fluorophore, *i.e*, $F_{RAA} = [\text{Fluoro } RA_2]/[\text{Fluoro}]$, $F_{RAB} = [\text{Fluoro } RAB]/[\text{Fluoro}]$ and $F_{RBB} = [\text{Fluoro } RB_2]/[\text{Fluoro}]$. Inherent in the above treatment is the underlying assumption that neither solvent component forms a non-fluorescent association complex with the fluorophore. If such complexation does occur, then Eqn. 13 describes only the fraction of the solute molecules that actually fluoresce.

Spectral properties for the solvational species RA_2 and RB_2 can be conveniently determined by measuring the fluorescence emission properties of the PAH probe molecule in both pure solvents. Properties for the mixed solvational fluorophore, on the other hand, must be estimated as it is impossible to isolate RAB since it must be in chemical equilibrium with both RA_2 and RB_2, in accordance with the proposed two-step solvational scheme. Emission intensities for RAB are approximated as the arithmetic average of intensities for RA_2 and RB_2, which is identical to the approximation invoked by Skwierczynski and Connors[11] in their interpretation of the spectral behavior of the Dimroth-Reichardt betaine dye dissolved in various binary aqueous-organic mixtures. Within this framework, examination of Eqn. 13 reveals that the observed PAH emission spectra for a binary solvent mixture is

$$\begin{aligned} \text{Spectrum (at } X_B) = {} & (F_{RAA} + 0.5\, F_{RAB})\ \text{Spectrum } RA_2 \\ & + (F_{RBB} + 0.5\, F_{RAB})\ \text{Spectrum } RB_2 \end{aligned} \quad (14)$$

a weighted average of the fluorophore's spectra in each of the two pure solvents, provided that the molar concentration of fluorophore remains constant for each series of measurements and that the molar extinction coefficients and fluorescent quantum yields of solvational species are independent of binary solvent composition. Emission intensities are additive at each wavelength. In the case of a PAH solvent polarity probe such as pyrene, the calculated I_1/I_3 emission intensity ratio (or I_1/I_2 in case of BePy) is

$$\begin{aligned} I_1/I_3 \approx {} & [(F_{RAA} + 0.5\, F_{RAB})\, I_{1,\text{solvent } A} + (F_{RBB} + 0.5 F_{RAB})\, I_{1,\text{solvent } B}] \\ & \div [(F_{RAA} + 0.5 F_{RAB})\, I_{3,\text{solvent } A} + (F_{RBB} + 0.5 F_{RAB})\, I_{3,\text{solvent } B}] \end{aligned} \quad (15)$$

also determined by the relative mole fractions of the three assumed solvational fluorophores, which in turn are related to the stoichiometric composition of the binary solvent mixture through Eqns. 3–5. Here, we have assumed that both the I and III band emission wavelengths are solvent independent, which is not strictly true, hence the approximately equal to sign is used. Rigorous applications require that intensity measurements be made at two fixed emission wavelengths.

Readers should note that basic spectroscopic principles state that emission intensities are additive. It can be shown that a similar expression holds for uv/visible absorption spectroscopy. In this latter case, absorbances are the additive quantity. Equation 13 clearly shows that there is no simple mathematical relationship to calculate the maximum absorption wavelength (or alternatively E_T) determined in binary mixtures from values in the pure solvents as implied in the Skwierczynski and Connors[11] data treatment (see Eqns. 6 and 8). From an operational standpoint, we feel that a better data treatment would have involved measuring the absorption spectrum of the Dimroth-Reichardt betaine dye in each pure solvent and in the various binary solvent mixtures. The absorption spectrum of the "postulated" mixed *RAB* solvational species could be approximated as having an intermediate general shape between Spectrum RA_2 and Spectrum RB_2, but with a maximum absorption wavelength of $(1/\lambda_{max})_{RAB} = 0.5[(1/\lambda_{max})_{RAA} + (1/\lambda_{max})_{RBB}]$, a maximum absorbance of $(A_{max})_{RAB} = 0.5[(A_{max})_{RAA} + (A_{max})_{RBB}]$, and a bandwidth of one-half A_{max} of $(\text{Width})_{RAB} = 0.5[(\text{Width})_{RAA} + (\text{Width})_{RBB}]$. "Optimized" numerical values of K_1 and K_2 could then be calculated via standard nonlinear regressional methods by substituting the three individual solvational spectrum into

$$\text{Spectrum (at } X_B) = F_{RAA}\,\text{Spectrum}\,RA_2 + F_{RAB}\,\text{Spectrum}\,RAB + F_{RBB}\,\text{Spectrum}\,RB_2 \tag{16}$$

and requiring that the resulting equation generate the observed dye absorption spectrum at each binary solvent composition. Thermodynamic models[31] can estimate the change in energy between the ground and excited states of RAB; however, this is conceptually different than predicting the maximum intensity wavelength that results from summation of three overlapping absorption/emission spectra. Spectroscopic principles govern the amount of radiation that is detected. Equation 14 applies only if the postulated *RAB* spectrum is an arithmetic average of the two pure solvation spectra. This particular approximation seems reasonable in the case of PAH solvent polarity probes since there is only a small redshift (circa $\pm$ 3 nm) in the emission wavelengths with increasing solvent polarity.

Application of Eqn. 15 is relatively straightforward if the spectrofluorometer is equipped with data processing and manipulation software. Depending upon the desired objective, one can compute either "optimized" values of the step-wise exchange constants for each PAH-binary solvent system studied, or "non-optimized" K_1 and K_2 values by solving simultaneously two equations of the form of Eqn. 15 using as input the observed I_1/I_3 emission intensity ratio determined at two different binary solvent compositions (e.g., $\Phi_A \approx 0.3$ and $\Phi_A \approx 0.7$) and measured $I_{1,\text{solvent}\,i}$ and $I_{3,\text{solvent}\,i}$ band intensities in both pure solvents. The latter method is

employed in the present study since it provides a more demanding test of the limitations and applications of the basic model in that the calculated spectrum for seven compositions represent outright predictions. Values of K_1 and K_2 are then substituted into Eqn. 14 to generate the calculated fluorescence emission spectra, which are compared to the observed data. Careful attention is given to ensure that the entire detailed emission fine structure (wavelengths and all intensity ratios) is correctly produced, rather than just the experimental I_1/I_3 ratio. Spectra *A* and *B* in Figure 2 represent the emission intensities of coronene dissolved in neat *n*-heptane and 1,4-dioxane, respectively, scanned from 420 to 520 nm. Values of $K_1 = 0.886$ and $K_2 = 0.178$ reproduced very accurately the observed coronene emission spectrum at a binary solvent composition of $\Phi_{\text{Heptane}} = 0.50$ after normalization to a common band intensity (spectrum C versus spectrum D in Figure 2). Normalization corrects for small differences in experimental conditions, such as fluorophore concentration, ambient temperature, and excitation source intensity, which may occur during any given series of fluorescence measurements. In most cases there was less than a 1% difference between the emission intensities for the observed and calculated normalized spectra at each wavelength scanned.

Table 1 summarizes results of our exchange constant computations for pyrene, benzo[ghi]perylene, benzo[e]pyrene, coronene, methylcoronene and 1, 2-dimethylcoronene dissolved in binary *n*-heptane + 1,4-dioxane and *n*-heptane + tetrahydrofuran

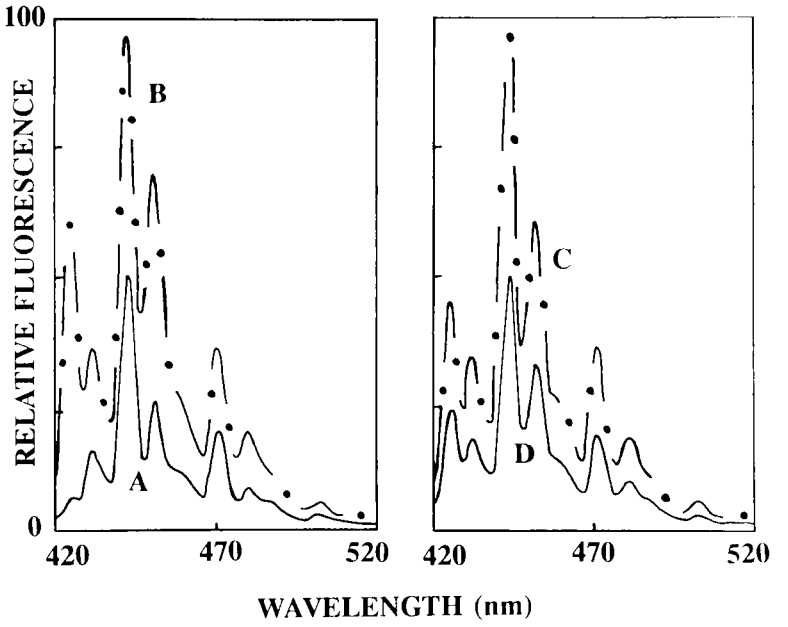

Figure 2 Fluorescence emission behavior of coronene dissolved in neat *n*-heptane (A, ————), in neat 1,4-dioxane (B, ——● ——), and in a binary *n*-heptane + 1,4-dioxane mixture (C, ——● ——) having a stoichiometric volume fraction composition of $\phi_{\text{Heptane}} = 0.50$. Spectrum D (————) represents the emission spectrum calculated using Eqns. 14 and 15, with step-wise exchange constants of $K_1 = 0.886$ and $K_2 = 0.178$. After normalization to a common band intensity, spectra C and D are superimposable.

Table 1 Step-wise Exchange Constants for the Khossravi-Connors Solution Model Calculated from Fluorescence Emission Properties of Polycyclic Aromatic Hydrocarbon Solutes.

PAH Solute Probe	K_1^a	K_2^a
n-Heptane (A) + 1,4-Dioxane (B)		
Pyrene	0.377	0.005
Benzo[e]pyrene	0.430	0.019
Benzo[ghi]perylene	1.350	0.267
Coronene	0.886	0.178
Methylcoronene	1.116	0.151
1,2-Dimethylcoronene	0.408	0.022
n-Heptane (A) + Tetrahydrofuran (B)		
Pyrene	0.666	0.127
Benzo[e]pyrene	1.439	0.485
Benzo[ghi]perylene	1.673	1.554
Coronene	1.747	0.898
Methylcoronene	2.554	0.798
1,2-Dimethylcoronene	1.926	0.716

[a] Numerical values of the two step-wise association constants were calculated using measured PAH fluorescence emission intensity ratios determined at binary solvent compositions of $\phi_{\text{Heptane}} = 0.3$ and $\phi_{\text{Heptane}} = 0.7$.

solvent mixtures. Comparison of the K_1 and K_2 values for the two cyclic ethers reveals that tetrahydrofuran is better at displacing *n*-heptane in the PAH solvational sphere than is 1,4-dioxane. This should not be too surprising considering the shapes of the cyclic ether cosolvents. Solutions generally mix so as to maximize strong, favorable molecular interactions and to minimize void volume. Void volume leads to inefficient molecular packing, and thus to a reduced number of molecular interactions. Very often the resulting distribution of molecules in solution is a compromise between these sometimes two competing effects. In the present case, 1,4-dioxane possesses a "chair-like" conformation, which is better at stacking on top of similar chair-like molecules than on top of a planar PAH molecule. The "open-flapped envelope" conformation of tetrahydrofuran is more compatible with the planar PAH ring system, and this explanation is borne out by the relative magnitude of the two sets of the step-wise exchange constants.

The effective local composition of *n*-heptane around the dissolved PAH flurophore is defined as the number of *n*-heptane molecules in all solvational species divided by the total number of solvational sphere molecules, i.e., $Y_{HP} = (2F_{RHpHp} + F_{RHpDx})/(2F_{RHpHp} + 2F_{RHpDx} + 2F_{RDxDx})$. Figures 3–5 graphically depict the degree of preferential solvation in the six *n*-heptane + 1,4-dioxane systems studied. The nine stoichiometric binary compositions are represented as mole fractions. Uncertainties assigned to the various Y_{Heptane} and $(1 - Y_{\text{Heptane}})$ values, indicated by error bars, were based upon the reproducibility of the emission intensity ratios (*circa* $\pm$ 0.02) and the range of K_1 and K_2 values that were obtained whenever the two input intensity ratios were increased/decreased by ± 0.02 from their correct experimental

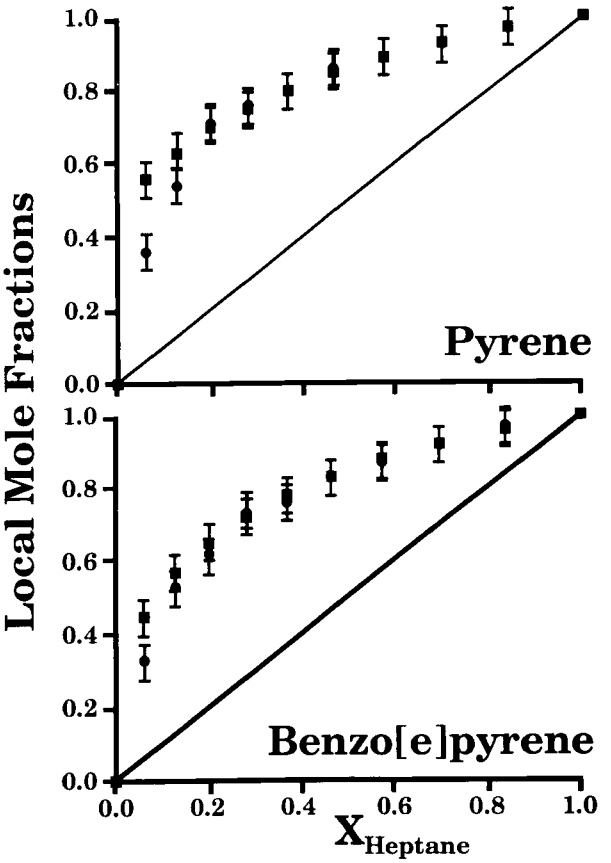

Figure 3 Preferential solvation of pyrene and benzo[e]pyrene dissolved in *n*-heptane + 1,4-dioxane mixtures. Numerical values of $Y_{Heptane}$ denoted as (•) and (■) were calculated from Eqns. 2 and 15, respectively, using the observed I/III (or I/II in the case of BePy) emission intensity ratios. The x-axis denotes the stoichiometric mole fraction composition of the binary solvent.

values. Superimposed on each figure are the local mole fraction compositions calculated from Eqn. 2 (denoted by •) to show that the Khossravi-Connors-Skwierczynski two-step model does give similar results to other spectrofluorometric probe methods published in the chemical literature.

Mathematical equivalence of the Khossravi-Connors-Skwierczynski model and Eqn. 2 may at first be surprising, since both models were based upon a completely different pictorial representation of preferential solvation. Equation 2 assumes that each dissolved PAH solute probe is solvated by only one type of solvent molecules, either by solvent *A* or by solvent *B*, whereas the Khossravi-Connors-Skwierczynski model also permits formation of mixed solvational species. Assuming for the moment that the solution contains a series of solvational complexes of the type of RA_iB_{z-i}, basic spectroscopic principles require that the observed fluorescence

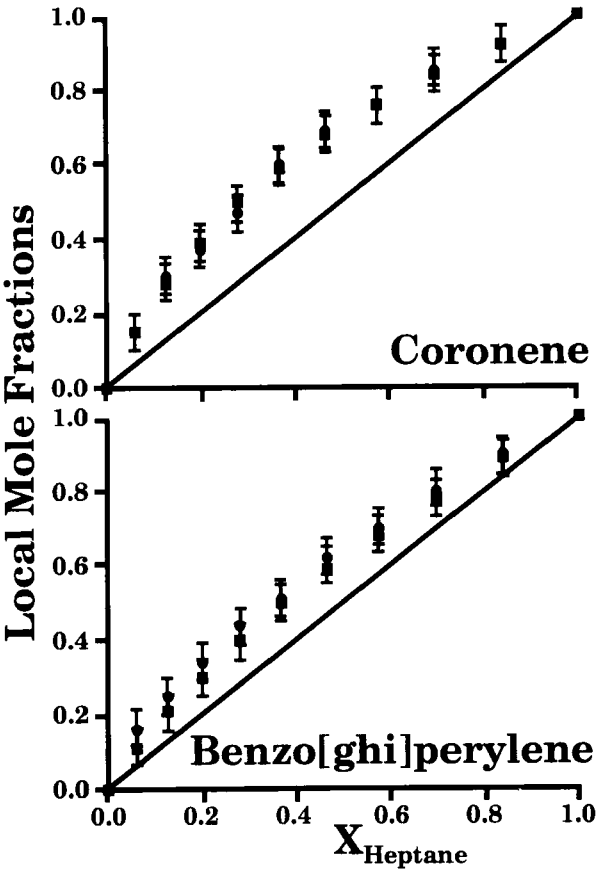

Figure 4 Preferential solvation of coronene and benzo[ghi]perylene dissolved in *n*-heptane + 1,4-dioxane mixtures. Numerical values of Y_{Heptane} denoted as (●) and (■) were calculated from Eqns. 2 and 15, respectively, using the observed I/III emission intensity ratios. The x-axis denotes the stoichiometric mole fraction composition of the binary solvent.

emission signal at each wavelength scanned be

$$F_{\text{obs}} = F_{RA_z} I_{RA_z} + \sum_{i=1}^{z-1} F_{RA_iB_{z-i}} I_{RA_iB_{z-i}} + F_{RB_z} I_{RB_z} \tag{17}$$

the fractional sum of emission intensity contributions from all species present in solution. For derivational simplicity we have defined z as the single coordination number for all solvational complexes (consistent with arguments put forth by Homer *et al.*[29,30]); however, this particular restriction can be relaxed without affecting the final outcome. Anytime that the fluorescence emission spectrum of RA_iB_{z-i} is approximated as Spectrum $RA_iB_{z-i} = (1/z)$ [i Spectrum $RA_z + (z-i)$ Spectrum

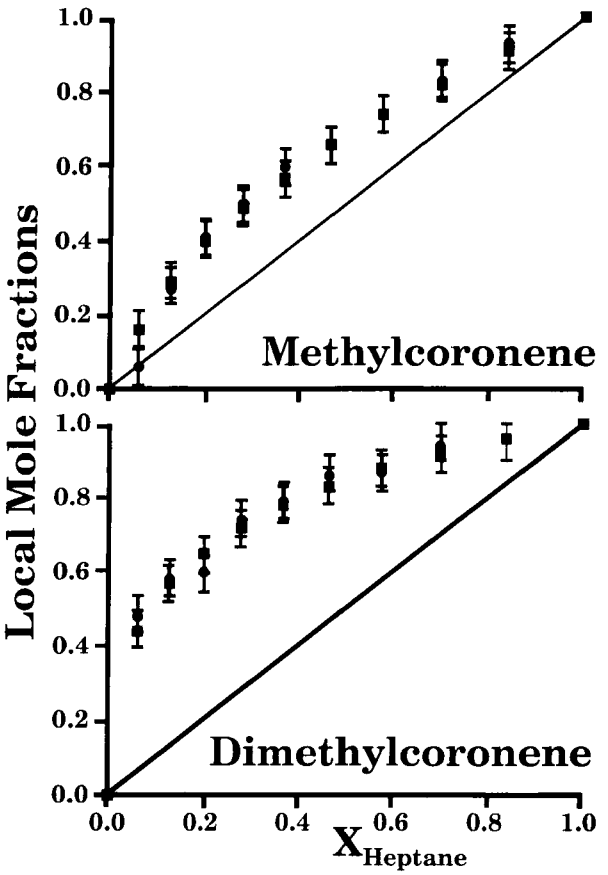

Figure 5 Preferential solvation of methylcoronene and 1,2-dimethylcoronene dissolved in *n*-heptane + 1,4-dioxane mixtures. Numerical values of Y_{Heptane} denoted as (●) and (■) were calculated from Eqns. 2 and 15, respectively, using the observed I/III emission intensity ratios. The x-axis denotes the stoichiometric mole fraction composition of the binary solvent.

RB_z], then the observed fluorescence emission signal can be rewritten as

$$F_{\text{obs}} = F_{RA_z} I_{RA_z} + (1/z) \sum_{i=1}^{z-1} i F_{RA_iB_{z-i}} I_{RA_z} + (1/z) \sum_{i=1}^{z-1} (z-i) F_{RA_iB_{z-i}} I_{R_z} + F_{RB_z} I_{RB_z}$$

$$= Y_A I_{RA_z} + (1 - Y_A) I_{RB_z} \tag{18}$$

where

$$Y_A = \frac{\left(z F_{RA_z} + \sum_{i=1}^{z-1} i F_{RA_iB_{z-i}} \right)}{\left(z F_{RA_z} + z \sum_{i=1}^{z-1} F_{RA_iB_{z-i}} + z F_{RB_z} \right)}$$

and I_{RA_2} is the measured PAH spectrum in pure solvent A. The above expression is mathematically identical to Eqn. 2. The reason that the two models returned different numerical values for Y_A at a few binary composition results entirely from the manner in which the models were applied. In Eqn. 2, Y_A values were computed from measured I_1/I_3 ratios at each of the nine possible binary compositions, whereas in the case of the Khossravi-Connors-Skwierczynski model the calculated K_1, K_2 and Y_A values were based upon only two of nine possible I_1/I_3 intensity ratios for each PAH-solvent system. Had we elected to optimize the two step-wise exchange constants, then there would have been ever better agreement between the Khossravi-Connors-Skwierczynski model and our previously derived Eqn. 2.

In closing, readers are reminded that it is fundamentally impossible to prove that a particular spectroscopic probe method is correct. One can demonstrate, however, that a given method is consistent with a wide range of experimental observations, which implies that the method and assumptions made therein may be correct. Similarly, it can be shown that a given spectroscopic probe method is inconsistent with experimental data so that the method must be either incorrect or incomplete. It is hoped that the ideas presented in this paper will prompt a critical re-examination of the relative merits of the various spectrofluorometric probe methods, Eqn. 2 versus Eqn. 15, in hopes of achieving a better understanding of solute-solvent interactions in fluid solution.

Acknowledgements

The authors thank J. C. Fetzer for kindly providing samples of methylcoronene and 1,2-dimethylcoronene S. A. Tucker acknowledges financial support from an American Chemical Society, Division of Analytical Chemistry Full-Year Fellowship sponsored by Glaxo, Inc.

References

1. P. Chatterjee and S. Bagchi, *J. Phys. Chem.*, **95**, 3311 (1991).
2. P. Chatterjee and S. Bagchi, *J. Chem. Soc., Faraday Trans.*, **86**, 1785 (1990).
3. M. Szpakowska and O. B. Nagy, *J. Chem. Soc., Faraday Trans.* 1 **85**, 2891 (1989).
4. W. P. Zurawsky and S. F. Scarlata, *J. Phys. Chem.*, **96**, 6012 (1992).
5. E. Bosch and M. Roses, *J. Chem. Soc., Faraday Trans.*, **88**, 3541 (1992).
6. P. Chatterjee and S. Bagchi, *J. Chem. Soc., Faraday Trans.*, **87**, 587 (1991).
7. K. Tamori, Y. Watanabe and K. Esumi, Langmuir, **8**, 2344 (1992).
8. D. J. Phillips and J. F. Brennecke, *Ind. Eng. Chem. Res.*, **32**, 943 (1993).
9. Y. P. Sun, G. Bennett, K. P. Johnston and M. A. Fox, *J. Phys. Chem.*, **96**, 10001 (1992).
10. W. E. Acree, Jr., S. A. Tucker and D. C. Wilkins, *J. Phys. Chem.*, **97**, 11199 (1993).
11. R. D. Skwierczynski and K. A. Connors, *J Chem. Soc., Perkin Trans.*, **2**, 467 (1994).
12. D. Khossravi and K. A. Connors, *J. Pharm. Sci.*, **81**, 371 (1992).
13. D. Khossravi and K. A. Connors, *J. Pharm. Sci.*, **82**, 817 (1993).
14. D. Khossravi and K. A. Connors, *J. Solution Chem.*, **22**, 321 (1993).
15. K. A. Connors, M. J. Mulski and A. Paulson, *J. Org. Chem.*, **57**, 1794 (1992).
16. K. A. Connors and D. Khossravi, *J. Solution Chem.*, **22**, 677 (1993).
17. R. F. Sullivan, M. M. Boduszynski and J. C. Fetzer, *Energy and Fuels*, **3**, 603 (1989).
18. K. W. Street, Jr. and W. E. Acree, Jr., *Analyst*, **111**, 1197 (1986).
19. D. C. Dong and M. A. Winnik, *Can. J. Chem.*, **62**, 2560 (1984).
20. R. Waris, M. A. Rembert, D. M. Sellers, W. E. Acree, Jr., K. W. Street, Jr., C. F. Poole, P. H. Shetty and J. C. Fetzer, *Appl. Spectrosc.*, **42**, 1525 (1988).
21. R. Waris, M. A. Rembert, D. M. Sellers, W. E. Acree, Jr., K. W. Street, Jr. and J. C. Fetzer, *Analyst*, **114**, 195 (1989).

22. R. Waris, K. W. Street, Jr., W. E. Acree, Jr. and J. C. Fetzer, *Appl. Spectrosc.*, **43**, 845 (1989).
23. W. E. Acree, Jr., S. A. Tucker, A. I. Zvaigzne, K. W. Street, Jr., J. C. Fetzer and H.-F. Grutzmacher, *Appl. Spectrosc.*, **44**, 477 (1990).
24. S. A. Tucker, A. I. Zvaigzne, W. E. Acree, Jr., J. C. Fetzer and M. Zander, *Appl. Spectrosc.*, **45**, 424 (1991).
25 W. E. Acree, Jr, S. A. Tucker and J. C. Fetzer, *Polycyclic Aromat. Cmpds.*, **2**, 75 (1991).
26. S. A. Tucker, W. E. Acree, Jr. and J. C. Fetzer, *Appl. Spectrosc.*, **49**, 8 (1995).
27. K. Nakashima and I. Tanaka, *Langmuir* **9**, 90 (1993).
28. S. M. Meyerhoffer and L. B. McGown, *Anal. Chem.*, **63**, 2082 (1991).
29. J. Homer and M. S. Mohammadi, *J. Chem. Soc., Faraday Trans., 2*, **83**, 1975 (1987).
30. J. Homer, M. H. Everdell, C. J. Jackson and P. M. Whitney, *J. Chem. Soc., Faraday Trans., 2*, **68**, 874 (1972).
31. W. E. Acree, Jr., D. C. Wilkins, S. A. Tucker, J. M. Griffin and J. R. Powell, *J. Phys. Chem.*, **98**, 2537 (1994).